ELSEVIER

Journal of Nuclear Materials 271&272 (1999) 450–454

journal of nuclear materials

Influence of helium on impact properties of reduced-activation ferritic/martensitic Cr-steels

R. Lindau [a], A. Möslang [a,*], D. Preininger [a], M. Rieth [a], H.D. Röhrig [b]

[a] Forschungszentrum Karlsruhe, Institut für Materialforschung, P.O. Box 3640, D-76021 Karlsruhe, Germany
[b] Projekt Kernfusion, P.O. Box 3640, D-76021 Karlsruhe, Germany

Abstract

Instrumented Charpy impact tests of the reduced activation type 8Cr2WVTa steel F82H have been performed after homogeneous implantation of 300 appm helium at 250°C. The results are compared with investigations on mixed spectrum neutron irradiated (HFR Petten) specimens. After neutron irradiation at 250°C to the same low damage dose of 0.2 dpa, the ductile–brittle transition temperature shift (ΔDBTT) amounts to 18°C, whereas a much higher ΔDBTT of 42°C has been measured after helium implantation. These results are compared with other neutron irradiated ferritic/martensitic steels having different boron levels and thus different helium contents. A model is proposed which describes the dynamic brittle fracture of martensitic/ferritic steels by a stress-induced propagation of micro-cracks, taking into account radiation induced hardening as well as helium bubble formation.

1. Introduction

Moving towards the development and world-wide optimization of reduced-activation 8–9Cr2WVTa steels, some encouraging results have become available meanwhile on the critical issue of low temperature irradiation induced hardening and embrittlement. Various data sets on neutron irradiated heats are showing that within wide temperature and displacement damage dose ranges this steel class is favorable also with respect to a general improvement of the fracture toughness properties [1–4]. However, whether helium generated by inelastic (n,α)-processes will have a significant effect on impact properties, such as the ductile–brittle transition temperature (DBTT), is subject of ongoing discussions [5–8]. The demonstration of a direct relationship between helium and embrittlement based on fast or mixed spectrum fission reactors is difficult because such simulation techniques require an alloying with B-10 or Ni-59 for the helium production.

This work describes changes in the Charpy impact properties of the reduced activation type 8Cr2WVTa steel F82H after homogeneous implantation of 300 appm Helium at 250°C. The results are compared with investigations on neutron irradiated specimens having the same damage dose of 0.2 dpa but a much smaller helium content of <8 appm. To explain the experimental results, a model is suggested that is able to distinguish between displacement damage induced hardening and He-embrittlement effects.

2. Experimental procedure

The chemical compositions of the ferritic/martensitic steels investigated in the current work is given in Ref. [9]. While the reduced activation steel F82H of type 8–9Cr2WVTa has been used for all Charpy tests, within the tensile test program the modified version F82H mod has been compared with the conventional steel MANET-1 of type 11CrMoVNb. The reference heat treatment following the specimen fabrication consisted of 1040°C/0.5 h + 750°C/2 h (F82H and F82H-mod), and 980°C/2 h + 1075°C/0.5 h + 750°C/2 h (MANET-1).

* Corresponding author. Tel.: +49-7247 82 4529; fax: +49-7247 82 4567; e-mail: anton.moeslang@imf.fzk.de.

0022-3115/99/$ – see front matter
PII: S 0 0 2 2 - 3 1 1 5 (9 8) 0 0 7 2 4 - 7

Instrumented charpy impact bending tests have been performed using an evaluation system for sub-size specimens according to the European standard ($3 \times 4 \times 27$ mm^3). The impact properties were characterized by the upper shelf energy (USE), the DBTT as well as the irradiation induced shifts of these values (ΔDBTT and ΔUSE). All charpy specimens used for the neutron and cyclotron irradiations are fabricated in the same manner. Details of the specimen fabrication, the neutron irradiation, and the instrumented Charpy tests are described elsewhere [10]. The helium implantation was performed at the cyclotron facility of FZK using a degraded 104 MeV alpha-particle beam. The irradiation conditions are given in Table 1. The irradiation temperature was measured with thin thermocouples of 0.1 mm diameter welded on the specimen surface outside the fracture zone and controlled by the flow rate of the surrounding helium gas atmosphere. During all irradiations the temperature stability was within ±1.5%. Special emphasis has been put on adjusting a fairly low helium implantation and damage production rates. It is important to note that in this specimen type the charpy tests derives all relevant information from the first third of the total crack surface (3×3 mm^2) behind the notch, as experimental tests and stress–strain analyses have shown [11]. Therefore, the limited alpha-particle range of 1.35 mm, resulting in a homogeneous helium concentration within 1.25 mm, is sufficient to describe the impact of helium implantation on charpy properties.

The tensile specimens with a reduced gauge volume of $7.0 \times 2.0 \times 0.20$ mm^3 were produced by spark erosion from foils with the gauge length parallel to the rolling direction. After irradiation the tensile specimens were tensile tested together with unirradiated control specimens at test temperatures equal to the irradiation temperature in a vacuum furnace ($\sim 10^{-4}$ Pa) at a constant nominal strain rate of $\dot{\varepsilon} = 1.2 \times 10^{-4}$ s^{-1}.

3. Experimental results

Fig. 1 shows the temperature dependence of the impact energy for the unirradiated, the neutron irradiated and the helium implanted F82H specimens. After neutron irradiation a DBTT of −50°C and a ΔDBTT of 18°C was observed, whereas the 300 appm He implanted F82H steel has significantly higher DBTT and ΔDBTT values of −26°C and 42°C, respectively. The helium concentration of <8 appm generated during the neutron irradiation results mainly from the ^{10}B burn-up. Assuming a comparable hardening efficiency of mixed spectrum neutrons and energetic alpha-particles, which is supported by the calculation of the PKA spectra of light ions taking into account non-elastically produced recoils [12], these results can be interpreted as a direct proof that under dynamic loading conditions and at lower irradiation temperatures, helium contributes sensitively to the embrittlement of ferritic/martensitic steels already at relatively small dpa doses.

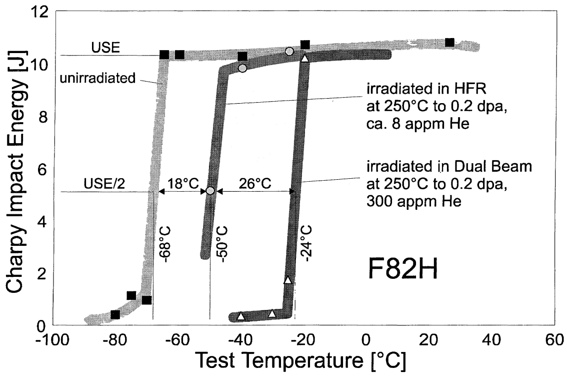

Fig. 1. Impact energy vs. test temperature curves showing the effect of displacement damage and helium in F82H.

As various observations in different neutron sources have shown, not only the helium content varies with the alloy composition but also the irradiation induced hardening as usually measured by means of tensile tests [13,14]. To determine whether the tensile properties are significantly affected by the presence of helium, F82H-mod and MANET-1 specimens were homogeneously helium implanted with 500 appm He at identical conditions. These two alloys have been chosen for the comparison mainly because the F82H-mod steel might be characterized among other properties by a very low boron content and a relatively small ΔDBTT, while MANET-1 has a high boron content and the highest ΔDBTT shift of all steels investigated. As Fig. 2 shows,

Table 1
Parameters of the alpha-particle cyclotron irradiations

	Charpy specimens	Tensile specimens
Irradiation temperature (°C)	250	60–550
Alpha-particle energy (MeV)	0–104	0–60
Damage rate (dpa/s)	$(4.4–7.3) \times 10^{-7}$	$(1.4–1.8) \times 10^{-6}$
He implantation rate (appm/s)	$(6–10) \times 10^{-4}$	$(2.5–3.0) \times 10^{-3}$
Damage dose (dpa)	0.22	0.30
He concentration (appm)	300	500

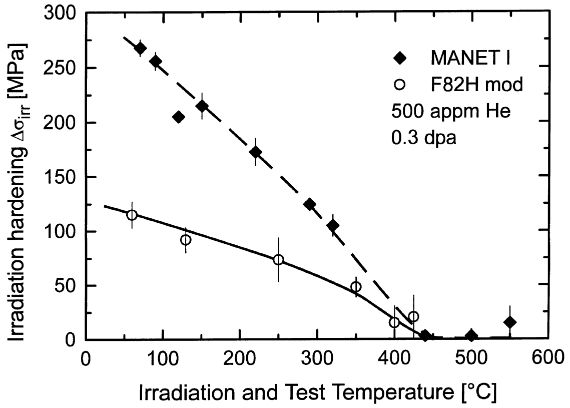

Fig. 2. Irradiation induced hardening vs. irradiation and test temperature of the steels F82H and MANET-1 following helium implantation.

after irradiation a strength increase has been observed in both steels that decreases continuously from 60°C to 350°C and diminishes rapidly above about 400°C. At 60°C e.g., this irradiation induced hardening $\Delta\sigma_{irr}$ amounts to 265 MPa in MANET-1 but only 115 MPa in F82H-mod specimens. Although tensile results at 0.3 dpa with a much smaller helium content are not yet available, it can be concluded from the similar helium concentration in both steels that helium quantity alone does not govern the strength properties. Instead, the dominant hardening contribution stems mainly from dislocation loops or displacement damage induced precipitation formation as the analysis of various strengthening contributions has shown for MANET-type steels [15]. Helium only contributes with a small part to strengthening. This is in agreement with the present body of knowledge from ferritic/martensitic steels, indicating that the helium induced strengthening might be in addition or conjunction with hardening from loops or precipitates by influencing their nucleation and growth [5–7]. However, a direct determination of the He-related hardening contribution in reduced activation ferritic/martensitic steels is still pending.

In a forthcoming paper TEM examinations are published that shows both after helium implantation and neutron irradiation very small helium bubbles nucleated often at dislocations and inner surfaces (e.g. precipitates).

4. Phenomenological embrittlement model and discussion

4.1. Model description

The dynamic quasi-cleavage fracture of tempered martensitic 7–12% Cr steels can be described at lower temperatures by stress induced micro-crack propagation [16,17]. As a consequence of the dynamic loading, stable multiple micro-cracking occurs within the plastic zone ahead of the crack tip. At high strain rates this unstable micro-crack propagation suppresses the concurrent ductile void nucleation, growth and coalescence mechanism. The void and micro-crack nucleation develop primarily at larger carbides (e.g. $M_{23}C_6$) or at lath and grain boundaries within a critical area ahead of the crack tip that can be characterized by the hydrostatic stress maximum. Cleavage fracture by unstable micro-crack propagation occurs if locally the material strength σ_{ε^*} exceeds the critical dynamic fracture stress σ_f^*. Thus, the condition

$$\sigma_{\varepsilon^*} \geqslant \sigma_f^* \tag{1}$$

is valid below the transition temperature DBTT and characterizes the regime of dynamic quasi-cleavage fracture. The achievement of the fracture stress σ_f^* is correlated with a critical local strain ε^* that initiates the unstable micro-crack propagation at a given critical micro-crack length l^*. Using Griffith's criteria, the fracture stress can be written as

$$\sigma_f^* = \sqrt{\frac{4E\gamma_{eff}}{l^*\pi}}, \tag{2}$$

where γ_{eff} is the effective interface energy dependent on plastic deformation and crack path. With this correlation the fracture stress depends on the microstructure by γ_{eff} and l^*, and on the temperature via the Young's modulus E. On the other hand the material strength $\sigma_{\varepsilon^*} = \sigma_0(\varepsilon^*) + \sigma_e(T, \dot{\varepsilon})$ can be characterized by the athermal part $\sigma_0(\varepsilon^*)$ and the temperature depending flow stress component

$$\sigma_e(T, \dot{\varepsilon}) = P\ \exp(-\beta_d T). \tag{3}$$

The parameter $\beta_d(\dot{\varepsilon})$ describes the temperature and strain rate behavior and P the Peierls stress, that is, the thermal flow stress at $T = 0$ K. With Eqs. (1)–(3) the transition temperature shift $\partial(\mathrm{DBTT})$ can be described by irradiation induced changes of $\sigma_0(\varepsilon^*)$ and σ_f^* [16]:

$$\frac{\partial(\mathrm{DBTT})}{\mathrm{DBTT}_0} = \frac{k_d}{P}\partial\big(\sigma_0(\varepsilon^*) - \sigma_f^*\big). \tag{4}$$

In general $k_d(\beta_d) \geqslant e$. However, tempered martensitic 7–12% Cr steels are near the broad minimum $\beta_d = 1/T_0$, where the boundary value $K_d = e$ can be used as good approximation. Allowing an irradiation induced change $\Delta\sigma_f^*$ of the fracture stress and using for the irradiation induced hardening

$$\Delta\sigma_{irr} = \Delta\sigma_{a,i} + \Delta\sigma_{a,\mathrm{He}} + \Delta\sigma_{e,i}, \tag{5}$$

the additive contributions $\Delta\sigma_{a,i}$ for athermal defects (e.g. loops, precipitates), $\Delta\sigma_{a,\mathrm{He}}$ for helium bubbles, and $\Delta\sigma_{e,i}$ for small defects which could be thermally activated (e.g. Frenkel pairs, defect clusters), Eqs. (2)–(5) can be written as

$$\frac{\Delta \mathrm{DBTT}}{\mathrm{DBTT}_0} \cong \frac{k_d}{P}\left[1+\frac{\Delta\sigma_{a,\mathrm{He}}-\Delta\sigma_\mathrm{f}^*}{\Delta\sigma_{a,i}}\right]\Delta\sigma_{a,i}. \qquad (6)$$

Because in our application $\Delta\sigma_{e,i}$ is much smaller than $\Delta\sigma_{a,i}$, the influence of $\Delta\sigma_{e,i}$ on k_d/P is also small. From Eqs. (4)–(6) follows, that the irradiation induced total shift ΔDBTT of the ductile–brittle transition temperature depends primarily on the transition temperature DBTT_0 of the unirradiated material, on the Peierls stress P as well as on the athermal stress contribution $\Delta\sigma_{a,i}$. The influence of σ_f^*, $\sigma_0(\varepsilon^*)$ and $\Delta\sigma_{e,i}$ on ΔDBTT, however, is much smaller. ΔDBTT is also independent of β_d, as long β_d remains constant. Altogether, the shift in the transition temperature can be characterized for individual alloys by plots showing $\Delta\mathrm{DBTT}/\mathrm{DBTT}_0$ versus $\Delta\sigma_{a,i}$. For such plots, the model predicts a linear to parabolic dependency.

At lower doses the irradiation hardening can be described fairly well by $\Delta\sigma_{a,i} \cong k_i\sqrt{\mathrm{dpa}}$, while the hardening of helium bubbles, might be given by $\Delta\sigma_{a,\mathrm{He}} \cong k_\mathrm{He}\sqrt{c_\mathrm{He}}/d_\mathrm{He}$ according to Orowan mechanism. k_i and k_He are temperature depending constants, c_He is the helium concentration and d_He the bubble diameter. In addition to this potential hardening contribution of helium, helium bubble decoration of fracture relevant inner surfaces ($M_{23}C_6$ precipitates, lath boundaries) reduces the fracture stress σ_f^* by lowering the interface energy according to Eq. (1). This embrittlement behavior can be taken into account by the expression $\sigma_\mathrm{f}^* \approx -k_{\mathrm{f,He}}\sqrt{c_\mathrm{He}^\mathrm{if}}$ in a phenomenological way, where $c_\mathrm{He}^\mathrm{if} = zc_\mathrm{He}$ is the fraction of helium on inner surfaces and $k_\mathrm{f,He}$ is a constant. With these assumptions, the irradiation induced shift of the DBTT should increase in martensitic Cr-steels at temperatures below about 350°C during the early stage of irradiation (a few dpa) in a linear way with $\sqrt{\mathrm{dpa}}$ and $\sqrt{c_\mathrm{He}/\mathrm{dpa}}$ until the quasi-saturation in the irradiation hardening $\Delta\sigma_\mathrm{irr}$ is reached. Beyond that limit, both $\Delta\sigma_\mathrm{irr}$ and the normalized shift $\Delta\mathrm{DBTT}/\mathrm{DBTT}_0$ increases only very moderate with damage dose. A more detailed derivation of the effect of irradiation and helium on embrittlement will be given together with a discussion of literature data in a forthcoming publication.

4.2. Discussion

Fig. 3 shows the irradiation induced increase of $\Delta\mathrm{DBTT}/\mathrm{DBTT}_0$ as a function of $\sqrt{\mathrm{dpa}}$ for the conventional 11CrMoVNb steel MANET-1 and for reduced activation 7.6–9.3CrWVTa steels following neutron irradiation at 300°C. The MANET-1 steel shows the strongest temperature shift and reaches at 5 dpa with a value of $\Delta\mathrm{DBTT}/\mathrm{DBTT}_0 \cong 1$ nearly saturation. The correlated proportional constants are $k_i \cong 201$MPa/(dpa)$^{-0.5}$ and $P = 900$ MPa. On the other hand the 7–10CrWTa steels, but also the 9Cr1MoVNb alloy, show a much smaller irradiation induced shift. With $\Delta\mathrm{DBTT}/\mathrm{DBTT}_0 \leqslant 0.3$ the F82H steel has the most favorable properties, and with $P \cong 1000$ MPa, $K_d = e$ the related coefficient k_i amounts to only 76.5 MPa/(dpa)$^{-0.5}$. These k_i-coefficients determined from Fig. 3 are compatible with the irradiation induced hardening $\Delta\sigma_\mathrm{irr}$ measured after cyclotron irradiation to 500 appm He and 0.3 dpa (Fig. 2).

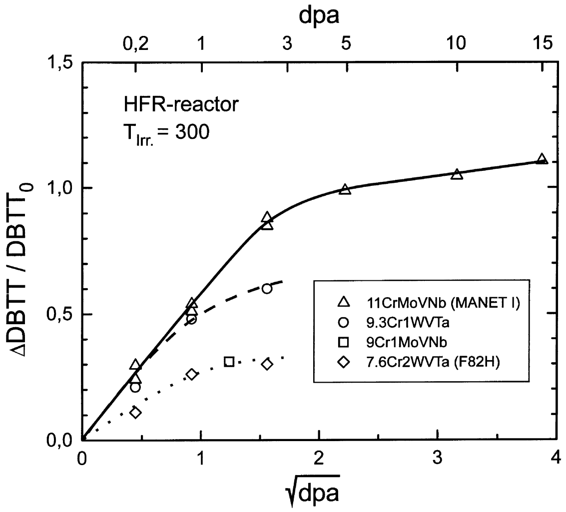

Fig. 3. Normalized shift of the ductile–brittle transition temperature vs. displacement damage of various martensitic steels following neutron irradiation at 300°C.

Fig. 4 shows for the MANET-1 steel the observed influence of the irradiation temperature T_irr on ΔDBTT/DBTT_0 after neutron irradiation to different damage doses. Obviously, ΔDBTT/DBTT_0 depends in accordance with the irradiation hardening $\Delta\sigma_\mathrm{irr}$ sensitively on irradiation temperature. It is important to note, that (i) in

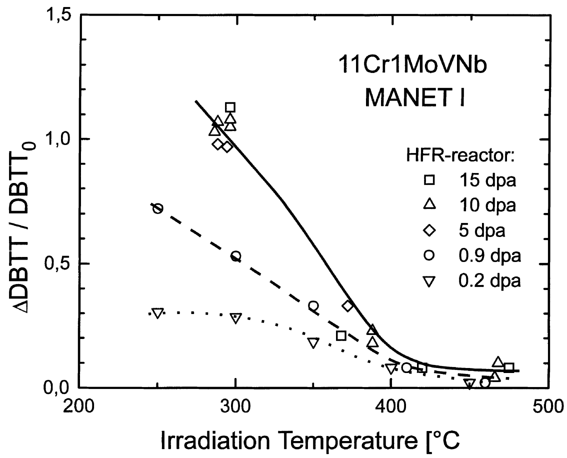

Fig. 4. Normalized shift of the ductile–brittle transition temperature vs. irradiation temperature of the MANET-1 steel.

spite of the relatively high helium content of 85 appm, ΔDBTT/DBTT$_0$ decreases above about 400°C to small values $\leqslant 0.1$, and (ii) although this helium production is almost completed at 1 dpa, ΔDBTT/DBTT$_0$ still increases significantly with damage dose below about 400°C until a quasi saturation level is reached. These observations emphasize that in the long run of neutron irradiations the displacement damage induced hardening rather than the helium content dominates the embrittlement.

5. Summary and conclusions

The experimental data of this work mainly based on MANET-1 and F82H irradiations have demonstrated that under dynamic loading conditions helium can contribute to the cleavage fracture embrittlement of martensitic steels. While in neutron irradiated specimens (low He/dpa ratio) the DBTT increase is mainly caused by displacement damage induced hardening, a significant fraction of the additional DBTT shift in helium implanted specimens (high He/dpa ratio) can be attributed to fracture stress reduction due helium segregation at fracture surfaces.

A phenomenological model is proposed that correlates the dynamic quasi cleavage fracture of martensitic steels with irradiation induced changes of the strength and of the fracture stress. Although micro-mechanical and micro-structural features are not yet included in detail, the model is able to distinguish quantitatively between helium and displacement damage induced embrittlement. It predicts that the relative shift in the ductile–brittle-transition temperature ΔDBTT/DBTT$_0$ should be basically proportional to the square root of the dpa dose and, in an additive manner, also to the square root of the helium.

Acknowledgements

The authors would like to express their appreciation to Professor K. Ehrlich for many helpful discussions. This work has been performed in the framework of the Nuclear Fusion Project of Forschungszentrum Karlsruhe and is supported by the European Union within the European Fusion Technology Program.

References

[1] A. Kohyama, A. Hishinuma, D.S. Gelles, R.L. Klueh, W. Dieth, K. Ehrlich, J. Nucl. Mater. 233–237 (1996) 138.
[2] K. Ehrlich, D.R. Harries, A. Möslang, FZKA report 5626 (1996).
[3] R.L. Klueh, G.J. Alexander, J. Nucl. Mater 233–237 (1996) 336.
[4] M. Rieth, B. Dafferner, H.D. Röhrig, C. Wassilew, Fusion Eng. Design 29 (1995) 365.
[5] R.L. Klueh, G.J. Alexander, J. Nucl. Mater. 218 (1995) 151.
[6] D.S. Gelles, J. Nucl. Mater. 230 (1996) 187.
[7] R.L. Klueh, G.J. Alexander, J. Nucl. Mater 230 (1996) 191.
[8] K. Shiba, M. Suzuki, A. Hishinuma, J. Nucl. Mater. 233–237 (1996) 309.
[9] M. Rieth, B. Dafferner, H.D. Röhrig, J. Nucl. Mater. 258–263 (1999) 1147.
[10] M. Rieth, B. Dafferner, W. Kunisch, H. Ries, O. Romer, FZKA report 5750 (1997).
[11] J.R. Griffiths, D.R.J. Owen, J. Mech. Phys. Solids 19 (1971) 419.
[12] E. Daum, J. Bertsch, A. Möslang, J. Nucl. Mater 233–237 (1996) 959.
[13] E. Materna-Morris, O. Romer, in: Fusion Technology 1994, K. Herschbach, W. Maurer, J.E. Vetter (Eds.), Elsevier, Amsterdam, 1995, p. 1281.
[14] R.L. Klueh, J.-J. Kai, D.J. Alexander, J. Nucl. Matter. 225 (1995) 175.
[15] A. Möslang, D. Preininger, K. Ehrlich, All-Union Conf. of the Effect of Irradiation on Materials of Fusion Reactors, St. Petersburg, Russian Federation, 18–20 September 1990.
[16] D. Preininger, Proc. of Materials week '96 (1997) 43 ISBN 3-88355-235-6.
[17] G.R. Odette, G.E. Lucas, in: P. Jung, H. Ullmaier (Eds.), Proceedings of the IEA Internat. Symposium on Miniaturized Specimens for Testing of Irradiated Materials, 22 September 1994, Forschungszentrum Jülich 1995, p. 160.